Leader neurons in population bursts of 2D living neural networks

2008 New J. Phys. 10 015011

(http://iopscience.iop.org/1367-2630/10/1/015011)

New Journal of Physics
The open-access journal for physics

Leader neurons in population bursts of 2D living neural networks

J-P Eckmann[1,2], Shimshon Jacobi[3], Shimon Marom[4], Elisha Moses[3,5] and Cyrille Zbinden[1]

[1] Département de Physique Théorique, Université de Genève, CH-1211 Genève 4, Switzerland
[2] Section de Mathématiques, Université de Genève, CH-1211 Genève 4, Switzerland
[3] Department of Physics of Complex Systems, The Weizmann Institute of Science, Rehovot 76100, Israel
[4] Department of Physiology and Biophysics, Faculty of Medicine, Technion, Haifa 31096, Israel
E-mail: elisha.moses@weizmann.ac.il

New Journal of Physics **10** (2008) 015011 (19pp)
Received 1 August 2007
Published 31 January 2008
Online at http://www.njp.org/
doi:10.1088/1367-2630/10/1/015011

Abstract. Eytan and Marom (2006 *J. Neurosci.* **26** 8465–76) recently showed that the spontaneous bursting activity of rat neuron cultures includes 'first-to-fire' cells that consistently fire earlier than others. Here, we analyze the behavior of these neurons in long-term recordings of spontaneous activity of rat hippocampal and rat cortical neuron cultures from three different laboratories. We identify precursor events that may either subside ('aborted bursts') or can lead to a full-blown burst ('pre-bursts'). We find that the activation in the pre-burst typically has a first neuron ('leader'), followed by a localized response in its neighborhood. Locality is diminished in the bursts themselves. The long-term dynamics of the leaders is relatively robust, evolving with a half-life of 23–34 h. Stimulation of the culture alters the leader distribution, but the distribution stabilizes within about 1 h. We show that the leaders carry information about the identity of the burst, as measured by the signature of the number of spikes per neuron in a burst. The number of spikes from leaders in the first few spikes of a precursor event is furthermore shown to be predictive with

[5] Author to whom any correspondence should be addressed.

regard to the transition into a burst (pre-burst versus aborted burst). We conclude that the leaders play a role in the development of the bursts and conjecture that they are part of an underlying sub-network that is excited first and then acts as a nucleation center for the burst.

Contents

1. Introduction

Neurons that are extracted from the brain before they form connections can be grown in a dish, where they proceed to build a random network that is different from the one that they make within the brain [1, 2]. As this network matures it spontaneously develops an electrical activity that is characterized by collective *bursts* [3–6]. The conceptual problems underlying spontaneous excitation of the network as a whole involve both the initiation and the propagation of the activity. Models of initiation usually rely on the existence of a constant level of random firing in the network, contributing to background noise that rises at times to a level that suffices to excite the network (e.g. [7]).

When the neurons are restricted to grow along lines, they create one-dimensional (1D) cultures and their firing pattern can be well understood in terms of a generation process that occurs in one of several burst initiation zones (BIZ), and a subsequent propagation from that area into the rest of the line [8, 9]. In 2D the situation is much less clear. While numerous studies identify BIZs in 2D as well, the course of the outward propagation is not concentric and is difficult to follow [3, 10–12]. Since signals are confined to propagate along the axons that are linear and not space filling, advance of the signal in the plane must be the collective effect of many neurons.

Eytan and Marom [13] recently found that in 2D a select group of neurons, termed 'first-to-fire' or 'precursor' neurons, begin to fire ahead of the rest of the network, and were found to do so consistently for the several hours that they were monitored. In this paper, we focus

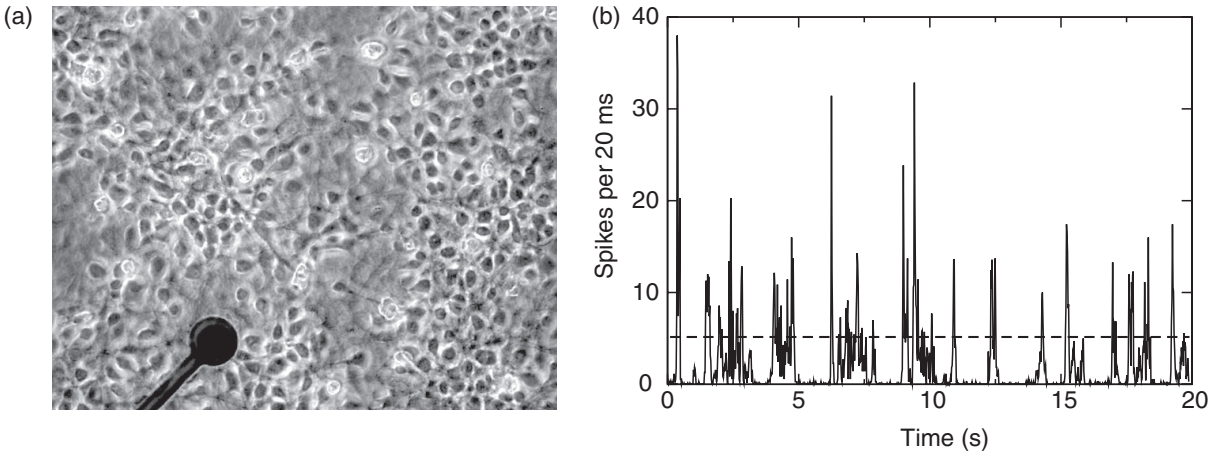

Figure 1. (a) 2D rat hippocampal neuron culture (*DF*) aged 14 DIV growing near one of the 60 measuring electrodes of the MEA. Electrode diameter is 30 μm. Phase micrograph taken using Zeiss Axiovert 135TV. (b) Example of spontaneous bursting activity from a *DF* culture aged 18 DIV. The number of spikes in 20 ms bins is drawn as a function of time. The dashed line demonstrates the burst detection threshold, which is 10 spikes in 40 ms.

on the properties of this group, asking first how general the phenomenon is. We do this by putting together data from different laboratories that were using different protocols. Beyond the importance of showing the generality of the phenomenon, its ubiquity gives a glimpse of questions related to initiation of the burst. Eytan and Marom (in figures 2 and 4(A) of [13]) identified the difference between 'aborted' and 'fully developed' bursts, and we show here that the leading group of neurons has the capacity to classify the fate of the upcoming network spike. Furthermore, we ask whether two bursts with different leading neurons are different. We shall show that although bursts are generally very similar to each other, there are leader-based 'classes' of network spikes that can be separated based on the statistics of electrode spiking.

The results of Eytan and Marom also raise several interesting questions regarding the role of the leading neurons in activating the network. Are these neurons simply better connected to the actual initiation zone, or are they part of it, and actively participate in creating and propagating the burst? Since the experiments are performed with multi-electrode arrays (MEA) that typically monitor only about 0.1% of the neurons in the culture, a further question is: how many such 'first-to-fire' groups exist in the whole culture and how do they interact with each other? The possibility of a 'sub-network' of such neurons that ignites the rest of the culture is an intriguing one.

In this study, we explore the collective mechanism for the initiation of the burst. Our approach will be to look first into the individual structure of each burst and to study the properties of the 'first-to-fire' neurons. We then ask whether and how their activity actually predicts properties of the burst that follows.

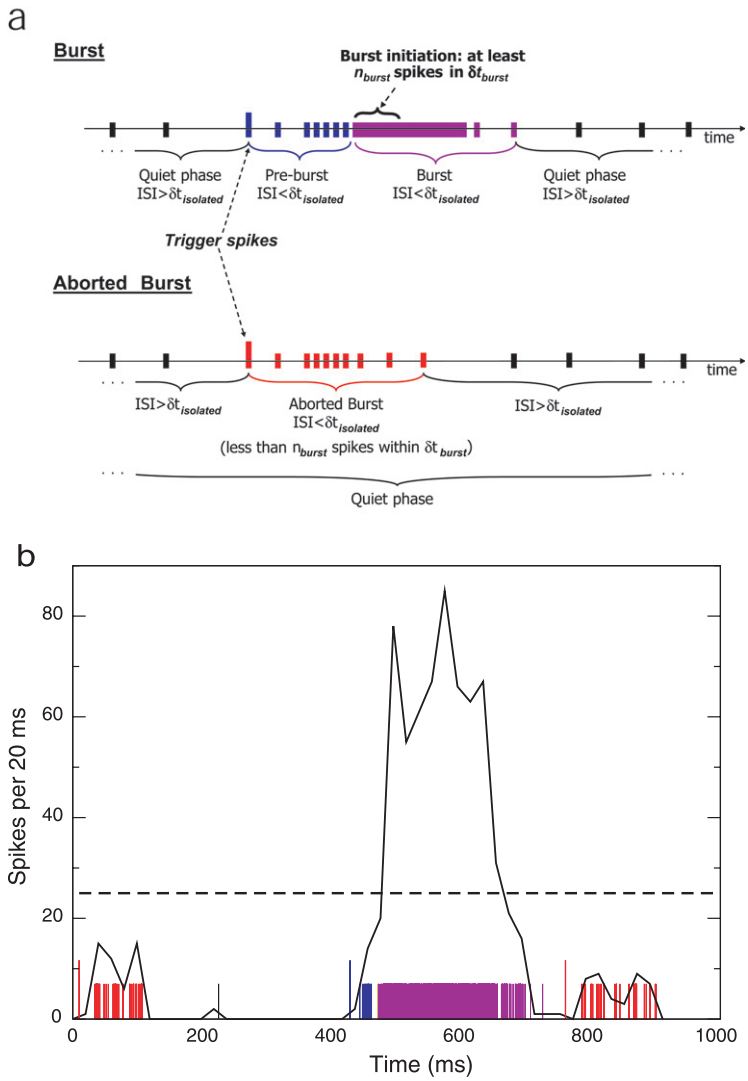

Figure 2. Burst identification. (a) A schematic drawing of the classification of spikes. The vertical lines indicate spikes, with the following color code: violet (burst), blue (pre-burst), red (aborted burst) and black (isolated events). Spikes with interspike interval (ISI) below $\delta t_{\text{isolated}}$ are grouped into a pre-burst that is followed by a burst if the spike density exceeds n_{burst} spikes in δt_{burst} (top timeline), or into an aborted burst otherwise (bottom timeline). (b) Example from data of spontaneous bursting activity in a *CF* culture. Single spikes are depicted as vertical lines with the color code as in (a), while the number of spikes per 20 ms bins is drawn as a line. This data set includes one *isolated spike*, two *aborted bursts* and one *burst* and its associated *pre-burst*. The trigger spikes are shown with a somewhat longer vertical line. The dashed line demonstrates the threshold value $n_{\text{burst}} = 25$ in $\delta t_{\text{burst}} = 20$ ms for *CF*.

Table 1. Culture types used in this work. $X \times Y$ are the array dimensions, D is the interelectrode distance and DIV stands for days *in vitro*.

Name	Feeding schedule	Source	Culture diameter (mm)	Feeding medium	Array size, $X \times Y$ (mm) and $D(\mu m)$	No. of cultures
CF [13]	Continuous perfusion from DIV 14	Rat cortical, postnatal day 1	15	5% horse serum	1.4×1.4 and 200	1
DF	33% medium replacement, daily	Rat hippocampal, prenatal day 19	15	10% horse serum	2.5×4.5 and 500	12
WF [6]	50% medium replacement, 5 days	Rat cortical, prenatal day 18	4	10% horse serum	1.4×1.4 and 200	4

2. Methods

2.1. Neural culture types

We analyzed the data from 2D cultures prepared in three different protocols taken in three different laboratories. They are classified according to their respective feeding protocols, which we found to be the most significantly differentiating parameter of the growth and preparation conditions:

- '*CF*' for a continuously fed culture, prepared from cortices of postnatal rats that are continuously perfused [13], from the Marom laboratory.
- '*DF*' for daily fed cultures, prepared from hippocampi of prenatal E19 rats, from the Moses laboratory, see figure 1.
- '*WF*' for cultures fed every 5–7 days, prepared from cortices of E18 rats [6], from the Potter laboratory.

The three culture types are compared in table 1.

2.2. Preparation and measurement of DF cultures

Here, we only describe the preparation of *DF* cultures. The preparation of *CF* is described in [13], and the preparation of *WF* cultures in [6].

2.2.1. MEA preparation. MEA of 6×10 electrodes with $500\,\mu$m spacing were used (MultiChannelSystems, Reutlingen, Germany). The MEA were prepared by using overnight application of PEI solution (Poly Ethylene Imine, Sigma, 0.05% in borate buffer). Two hours prior to cell plating, the MEA were washed four times with double-distilled water and left with plating medium.

2.2.2. Culture preparation and maintenance. Rat hippocampal neurons were taken from embryos of 19-day pregnant Wistar rats. The dissection and plating were done according to [14, 15], with daily feeding of the culture. Briefly, the hippocampus was mechanically dissociated, and cells were plated at a concentration of 12 000 cells mm^{-2} in 3 ml of plating medium (5% fetal calf serum (FCS; Sigma) and 5% heat-inactivated horse serum (HIHS; Sigma) in Eagle's MEM (Sigma) enriched with 0.6% glucose, Glutamax (Invitrogen) and 15 mg ml^{-1} Gentamicin (MEM+3 g), enriched with 50 μl B-27 supplement). On day *in vitro* (DIV) 3–6, the culture was fed daily with 1 ml of changing medium, which consists of MEM+3 g, 5% FCS, 5% HIHS with 20 mg ml^{-1} 5-fluoro-2-deoxyuridine and 50 mg ml^{-1} uridine (both from Sigma), and from then on the culture was fed with 1 ml of final medium, which includes MEM+3 g with 10% HIHS. The resulting neuron density is about 2000 cells mm^{-2}.

2.2.3. Culture measurement. Measurements were performed at 37 °C, in a dry 5% CO_2 incubator. To minimize evaporation of the growing medium, the culture chambers were covered with a thin Teflon foil [16]. For each culture, we measured regularly and in a continuous way the spiking activity every 24 h, in DIV ranging from 5 to 41. The measurements for each culture were performed over times ranging from 1 to 24 h, from which extracts lasting 20–30 min were analyzed. Measurements which occurred less than 15 min after moving the culture or less than 6 h since the last feeding were discarded. Special care was taken to assure minimization of water loss from the growing medium [15, 17].

2.2.4. Spike detection. The detection was done following [15]. The output from the MEA1060 amplifier (×1000, MultiChannelSystems) was sampled at 20 kHz (PCI-6071E, National Instruments, Austin, TX). The condition for spike detection was that the absolute value of the sampled signal exceeds the threshold for at least 0.2 ms. The threshold was set at the maximum of 15 μV (voltages given are pre-amplification) and 3 times the signal standard deviation (SD) (which is ∼3.5 μV). Further spikes with opposite polarity and less than 3 ms apart were disregarded as they were usually caused by overshoot. Spike shape discrimination was not performed, so that the analysis relies only on the spike timing and the electrode position. The number of neurons recorded from each electrode was estimated separately by spikes sorting as 1–4, with an average of 2.5.

2.2.5. Culture stimulation. We used electric stimulation to modify the leader distribution, in two methods. The first method used one of the recording electrodes, to which a 0.6–1 V amplitude, 1 ms bipolar pulse pair with 10 ms interpulse interval was injected. The second method was bath stimulation, where two platinum electrodes were immersed in the growing medium 4 mm away from the electrode array center. The bath stimulation was not carried out directly over the electrode array to minimize the measurement dead time caused by the stimulation current. The electrodes were 10 mm of exposed wire, spaced 2.5 mm apart and were less than 1 mm above the neuron level. In this case, bipolar pulses with an amplitude of 2–3.5 V and a width of 20 ms were used.

For both methods, we used a battery-powered current source which is isolated from the surrounding environment to minimize electrical noise in the multi-electrode measurement. The culture was monitored in order to verify its response to the stimulation. The voltage of the

stimulation was adjusted to cause a culture-wide response in at least 50% of the stimulations when the stimulation frequency was set to the spontaneous bursting frequency.

2.3. Data analysis

2.3.1. Time course. Cultures were observed on DIV 5–41 or parts within. Measurements were taken typically once a day, during on the order of an hour. Each daily data set is termed *epoch*. There were on average 8, 25 and 20 epochs in *CF*, *DF* and *WF* cultures, respectively. We looked for changes of behavior across epochs, typically finding changes towards the middle of the measurement period. This naturally leads to a division of the epochs into two *superepochs*. Electrodes were included in the analysis of a given epoch ('active electrode') if they fired at least once in this epoch.

2.3.2. Definition of bursts and their triggers. The definition of bursts is based on the list of spikes that are obtained in the measurements. For each spike i, the list gives us t_i, the time of the ith spike, and E_i, the electrode on which that spike was measured.

We first divide all the spikes into four classes: *in-burst*, *pre-burst*, *aborted burst* and *isolated*, with each spike belonging to one and only one class. The precise definitions are given below, but basically a spike is in a burst if it is in a group of many spikes that follow each other closely. It is in a pre-burst or aborted burst if it is not in a burst but is in a sequence of spikes that are close enough in time so that communication between them is still possible. The distinction between pre-burst and aborted burst depends on whether the spike is eventually followed by a burst or not. Finally, all other spikes are isolated. The reader may want to refer to figure 2 for the definitions which follow.

More precisely, we use three parameters, $n_{\mathrm{burst}}, \delta t_{\mathrm{burst}}$ and $\delta t_{\mathrm{isolated}}$. We first look for interspike gaps of length at least $\delta t_{\mathrm{isolated}}$, and divide the set of all spikes into disjoint subsets $\mathcal{R}_m$ of consecutive spikes, where m is a running index. The $\mathcal{R}_m$ have the property that if i and $i+1$ are in $\mathcal{R}_m$ then $t_{i+1} - t_i \leqslant \delta t_{\mathrm{isolated}}$, while if $i \in \mathcal{R}_m$ and $i+1 \in \mathcal{R}_{m+1}$ then $t_{i+1} - t_i > \delta t_{\mathrm{isolated}}$. The rationale is that if the interspike gap is so large that no 'memory' could remain between the spike at t_i and the one at t_{i+1} (i.e. $t_{i+1} - t_i > \delta t_{\mathrm{isolated}}$), then the spikes belong to separate subsets.

We now want to further divide each $\mathcal{R}_m$ into the burst itself, characterized by a high density of spikes, and its precursor, which immediately precedes it in time but has a lower density. Each of the $\mathcal{R}_m$ contains at least 1 spike, but may contain many, and we subdivide it into two disjoint sets $\mathcal{R}_m = \mathcal{P}_m \cup \mathcal{B}_m$ (each of which can be empty). We first look for a spike that is followed by at least $n_{\mathrm{burst}} - 1$ spikes in $\mathcal{R}_m$ within a lapse of time $\delta t_{\mathrm{burst}}$. Denoting this spike's index by $i_* = i_*(m)$, this is the first index in $\mathcal{R}_m$ with the property:

$$t_{i_*+n_{\mathrm{burst}}-1} - t_{i_*} < \delta t_{\mathrm{burst}}. \tag{1}$$

The indices i_* up to the last index in $\mathcal{R}_m$ then make up the burst $\mathcal{B}_m$.

If the condition equation (1) is never met in $\mathcal{R}_m$, then $\mathcal{B}_m$ is empty, and the set $\mathcal{R}_m = \mathcal{P}_m$ is not subdivided and is called an *aborted burst* if it has more than 1 spike and is an *isolated spike* otherwise.

For those m where such an i_* can be found, we check if it is also the first spike in $\mathcal{R}_m$. If so, then that burst is an immediate burst that has no pre-burst, so that $\mathcal{R}_m = \mathcal{B}_m$. For all the other bursts (these are the majority), we divide $\mathcal{R}_m = \mathcal{P}_m \cup \mathcal{B}_m$, where $\mathcal{P}_m$ are the indices $i \in \mathcal{R}_m$ with

Table 2. Burst detection parameters.

Culture type	n_{burst}	δt_{burst} (ms)	$\delta t_{\text{isolated}}$ (ms)
CF	25	20	20
DF	10	40	50
WF	20	20	10

$i < i_*$, and $\mathcal{B}_m$ are the others. The letter $\mathcal{P}$ refers to pre-burst or aborted burst and $\mathcal{B}$ refers to burst.

Between bursts the activity is much lower, and we define these periods as *quiet periods*. Each quiet period, denoted $\mathcal{Q}_b$, for a running index b, is actually a concatenation of consecutive $\mathcal{R}_m$s that did not contain a burst in the earlier stage, or else an empty set. We now renumber the set of indices as follows:

$$\{1, \ldots, N\} = \mathcal{Q}_1 \cup \mathcal{P}_1 \cup \mathcal{B}_1 \cup \mathcal{Q}_2 \cup \mathcal{P}_2 \cup \mathcal{B}_2 \cup \ldots,$$

with $\mathcal{B}_b$ the bth burst, $\mathcal{P}_b$ the corresponding pre-burst (if it exists) and $\mathcal{Q}_b$ the corresponding quiet phase. We define the *trigger* of burst b as the electrode E_{i_b}, where i_b is the number of the first spike in $\mathcal{P}_b$ (respectively $\mathcal{B}_b$ if $\mathcal{P}_b$ is empty).

While $\mathcal{Q}_b$ may not contain any spike, we can always define a quiet duration. This duration is the time between the last spike of $\mathcal{B}_{b-1}$ and the first spike of $\mathcal{P}_b$ (respectively $\mathcal{B}_b$ if $\mathcal{P}_b$ is empty). The length of the quiet phase $\mathcal{Q}_b$ is therefore $t_{i_b} - t_{\hat{i}_{b-1}}$ ($>\delta t_{\text{isolated}}$), where i_b is the first spike in $\mathcal{P}_b$ (respectively $\mathcal{B}_b$ if $\mathcal{P}_b$ is empty), i.e. the trigger of burst b and $\hat{i}_{b-1}$ is the last spike of $\mathcal{B}_{b-1}$. We define T as the combined length of the quiet phases over the whole measurement. Therefore,

$$T = \sum_b t_{i_b} - t_{\hat{i}_{b-1}}$$

is the total duration of all quiet phases.

The parameters which were used for the three cultures are shown in table 2. An example of the data and the resulting spike classification is shown in figure 1(b).

With these definitions we can do now some statistics. The bursts actually do not carry much information, since practically all the electrodes are active, and so we focus on the activity of the system *outside* the bursts, with an emphasis on the pre-bursts. The question we ask is whether certain electrodes are the triggers of the neural activity more often than warranted by simple statistical expectation.

We start by estimating the expected rate (or spiking density) for each electrode. Two choices can be used here: averages over the $\mathcal{Q}_b$ or averages over $\mathcal{Q}_b$ and $\mathcal{P}_b$. Let us continue with the first option, which is the one used in our analysis.

For each electrode E_n, we define e_n as the number of times that E_n has spiked in the set

$$\mathcal{Q} = \mathcal{Q}_1 \cup \mathcal{Q}_2 \cup \ldots,$$

whose total duration is the T defined above. The rationale here is that some electrodes spike only in the bursts, but electrodes that are able to be triggers are those which can spike in the quiet phase. However, we have checked that for most electrodes the participation rate in the quiet phase is comparable to that in the bursts (data not shown).

2.3.3. Leaders. For every pre-burst, aborted burst or immediate burst, the electrode which fires first is the trigger. Since we are interested in their special role, we first need to make sure that triggers are not just electrodes with high activity, which therefore are statistically more often the first ones to fire. The following discussion will show that they are over-proportionally more often triggers.

Henceforth we only discuss bursts with a pre-burst and their triggers. To qualify as a leader, we require that a trigger's probability to lead bursts should be significantly higher than its probability to fire in the low-rate (quiet) intervals. Let M be the total number of bursts that have a pre-burst. We consider a spike in the quiet interval and term as q_n the probability that electrode E_n has fired that spike: $q_n = e_n / \sum_{n'} e_{n'}$. The probability for electrode E_n to be a spurious or random trigger F times is given by $P_n(F)$:

$$\binom{M}{F} q_n^F (1-q_n)^{M-F}.$$

In the limit of large M and reasonable q_n, this distribution is approximated by a Gaussian of mean Mq_n and variance $Mq_n(1-q_n)$. On the other hand, we denote by f_n the actual number of bursts with a pre-burst that electrode E_n leads (note that $\sum_n f_n = M$).

Thus we have a scale on which to test triggering. We define α_n, a 'leadership score', and decide that an electrode is a **leader** if it scores at least 3 SD above the natural expectation value. This corresponds to a p-value of 0.001. The criterion for leadership of electrode E_n is therefore

$$\alpha_n = \frac{f_n - Mq_n}{\sqrt{Mq_n(1-q_n)}} > 3.$$

A second condition is aimed at eliminating the electrodes that fire very seldom and lead a negligible number of bursts but are not screened by the first (statistical) condition. In practice, we exclude an electrode from being a leader if the fraction of bursts it leads is less than a threshold of 3% of the bursts.

2.3.4. Mutual information. We estimate the mutual information of two electrodes in a series of time intervals based on empirical probabilities, according to [18]. Using the division of time into pre-burst and burst intervals, we define a firing event in a given interval as $k = 0, 1$, where 0 stands for no spike and 1 stands for at least 1 spike. We did not use the quiet interval for this analysis. We denote by $N_n(k)$ the number of times electrode E_n had an event k in a series of N_{int} intervals. The probability assigned to event k is thus $p_n(k) = N_n(k)/N_{\text{int}}$. The number of joint events in which electrode E_n had event k_1 and electrode $E_{n'}$ had event k_2 is given by $N_{n,n'}(k_1, k_2)$. The joint probability of events k_1, k_2 for electrodes $E_n, E_{n'}$ is then given by $p_{n,n'}(k_1, k_2) = N_{n,n'}(k_1, k_2)/N_{\text{int}}$. The mutual information between two electrodes is then given by

$$I_{n,n'} = \sum_{k_1,k_2 \in \{0,1\}} p_{n,n'}(k_1, k_2) \cdot \log \frac{p_{n,n'}(k_1, k_2)}{p_n(k_1)\, p_{n'}(k_2)}.$$

3. Results

3.1. Neural activity

All three culture types showed spontaneous bursting in most of the active electrodes. In the cultures from all sources *CF* (a single culture), *DF* ($N = 9$ cultures) and *WF* ($N = 5$ cultures), the average rate of spikes per electrode per unit time gradually increased along the first 3 weeks of measurement period as did the bursting rate. The measurement period was (in DIV) 14–25 (*CF*), 5–41 (*DF*) and 5–30 (*WF*). The electrode firing rate (in hertz per active electrode) was 3–10 (*CF*), 1–3 (*DF*) and 4–10 (*WF*). For all cultures, more than 85% of the intact electrodes were firing together in bursts after DIV 14.

The main difference between the activities of the cultures lies in the rate of firing. In particular, maximal bursting rates were (in hertz) 1.6 (*CF*), 0.3–1.4, with an average of 0.65 (*DF*), and 0.07–0.84, with an average of 0.26 (*WF*). These maximal rates were obtained in ages of DIV 19–24 (*CF*), 14–21 (*DF*) and 21–28 (*WF*). The difference between the bursting rates can mainly be attributed to the feeding differences—we have seen that more frequent feeding increases the bursting rate [15]. By the third week-*in-vitro* of the culture, about 90% of the spikes were within bursts for all three culture types.

WF cultures were special in that they contained fewer bursts but were more active in the quiet intervals between the bursts, with an average firing rate (excluding bursts) of about 0.1 Hz per electrode as compared to 0.002 Hz (*DF*) and 0.02 Hz (*CF*).

3.2. Existence of leaders

Most of the bursts originated in a pre-burst (94% for *CF*, 86% for *DF* and 73% for *WF* cultures).

The pre-burst lasted on average 230 ms in *DF*, 180 ms in *CF* and 22 ms in *WF*. The average number of participating electrodes was 10 in *DF*, 18 in *CF* and 6 in *WF*. The bursts lasted on average 500 ms in *DF*, 314 ms in *CF* and 228 ms for *WF*. The corresponding average number of firing electrodes was 29 in *DF*, 48 in *CF* and 31 in *WF*.

Averaging over epochs, we find that 4 ± 1.9 (mean $\pm$ SD), 2.9 ± 1.2 and 2.0 ± 1.4 electrodes were leaders for more than 24 h in *CF*, *DF* and *WF* cultures, respectively.

3.3. Time evolution

We are interested in finding out whether leadership is maintained over successive epochs. It turns out that for all cultures the most significant leaders are indeed stable over multiple epochs, see figure 3. To quantify the leadership inertia, we define L_n as the set of epochs in which electrode n is a leader, i.e.

$$L_n = \{j \,|\, \alpha_{n,j} > \alpha_c\},$$

where $\alpha_c = 3$ is the threshold leadership score, and $\alpha_{n,j}$ is the leader score for electrode n in epoch j. If we define t_j^0 as the beginning of epoch j, then for every uninterrupted sequence $j', j'+1, \ldots, J$ of integers in L_n, we define the lifetime of leadership by $t_{J+1}^0 - t_{j'}^0$.

The *distribution* of the lengths of all these time intervals follows an exponential distribution with half-life (in hours) of 23.1 ± 3.0 (mean$\pm$SE) (*CF*), 34.4 ± 4.4 (*DF*) and 29.5 ± 3.6 (*WF*).

The difference between the culture types is probably caused by the culture maintenance protocol.

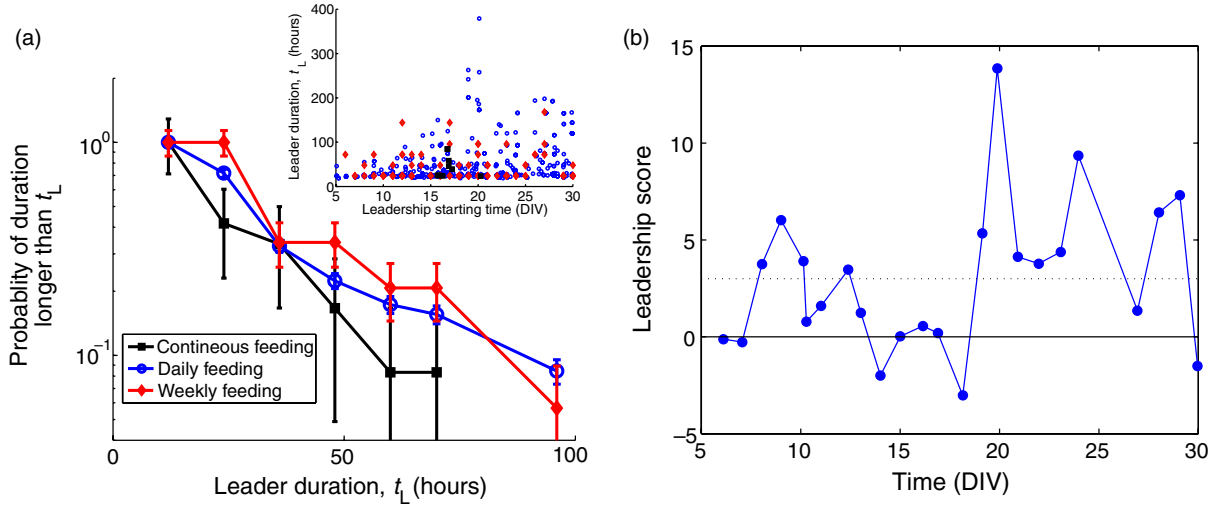

Figure 3. Leader electrodes remain with a high leadership score for days. (a) The distribution of the leadership duration, for the three culture types: *CF*, with continuous feeding (black squares); *DF*, with daily feeding (blue circles): and *WF*, with semiweekly feeding (red diamonds). Inset: leadership time durations of all leaders remaining at least 18 h, as a function of the leadership starting time (marker code as in (a)). (b) Leadership score as a function of DIV, for a typical leader electrode of *DF*.

3.4. Locality of activity

We assess the locality of electrode co-activation within the same burst or pre-burst, by measuring the mutual information as a function of distance. We compare the pre-burst to the burst, and show that activity in the pre-burst is localized while the activity in the burst tends to spread all over the culture. We quantify the tendency to fire together by estimating the mutual information between electrode pairs as described in section 2. A pair of electrodes has higher mutual information if they participate in the same pre-burst or burst interval. We plot the mutual information $I_{n,n'}$ as a function of $d_{n,n'}$, the distance between the electrodes n and n', averaging over all electrode pairs which have the same distance. The mutual information decreases with the interelectrode distance for all interval types. In the pre-burst, we get a reasonable exponential fit of the form $I(d) = A \exp(-d/D)$, see figure 4.

The value of D in the pre-burst interval can be measured reliably in epochs of maximal activity, occurring in DIV 19–23 (*CF*), 10–20 (*DF*) and 15–24 (*WF*). At other times, the decay is too small to calculate D reliably. On these days, D (in millimetres) of the pre-burst interval either wanders between 0.64 and 1.8 as a function of culture age (*CF*) or takes constant values of 1.85 ± 0.16 (*DF*) and 1.09 ± 0.02 (*WF*). In all epochs of maximal activity defined above, the localization in the burst interval as well as in the quiet phase is weaker than in the pre-burst interval.

The actual values of the mutual information displayed in figure 4 are of interest. The mutual information in the burst is typically 5 times higher than in the pre-burst. This shows that in the burst, the co-activation is much higher than in the pre-burst. Looking at figure 4, one can see that in the pre-burst the mutual information decays gradually, going to zero at long distances.

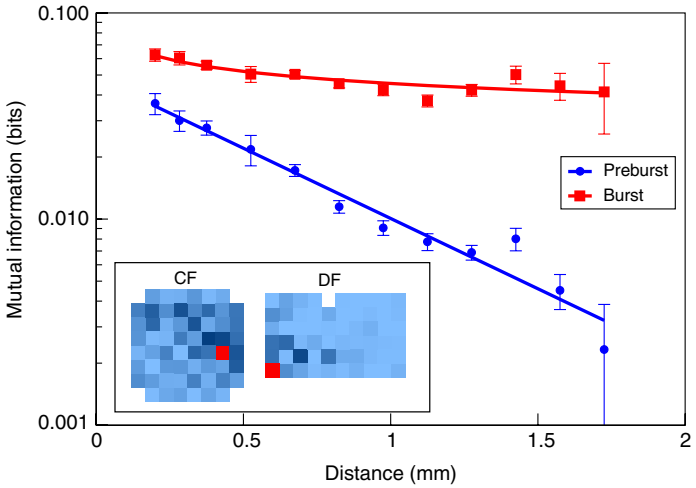

Figure 4. Average mutual information (MI) as a function of distance for pre-burst and burst intervals. An example is given for the *CF* culture, at an age of 22 DIV. The activity landscape is more localized in the pre-burst, and is fitted by an exponential with a length scale of 0.67 mm (blue line, $R = 0.97$). The landscape in the burst is relatively flat, the length scale is higher and the mutual information is fitted by a power law, MI$\sim d^{-0.12}$ (red line, $R = 0.90$). Inset: probability of electrodes to fire together in a pre-burst for two sample cultures, and for a sample leader in each culture. Leaders are denoted in red, and the color code is light blue for low activity and dark blue for high activity.

In contrast, during the burst, it has a short initial decay, in the order of 1–2 mm, beyond which the information is maintained at a constant value. We conclude that in the pre-burst the activity is primarily local, decaying to zero within a few millimetres. In contrast, in the burst the local effect is limited (within 1 mm), and once the burst develops and advances outside this local region all of the culture behaves as one correlated region.

As it is known that the recruitment of neural activity in bursts is based on synaptic transmission [1, 4], we relate the correlation length to the number of synaptic connections that the signal must propagate through. This in turn is determined by the axonal length, which is also in the range of about 1 mm in similar cultures [19, 20].

3.5. Effect of stimulation

We have seen that the leaders can remain stable over long times when the culture is spontaneously active. We wished to assess whether the leaders can be changed using an external driving force [21]. In order to modify the leader distribution, we stimulated the cultures using either one of the MEA electrodes or bath electrodes (see section 2). These experiments were only done on three *DF* cultures, in addition to the nine cultures discussed above. The stimulation was repeated 40–240 times, in stimulation frequencies of 0.2–1 Hz during periods of 2–5 min for bath stimulation, and 500–1000 times in frequencies of 0.1–0.3 Hz during periods of 20–30 min for single-electrode stimulation. The response of the culture to the stimulation did not exceed the spontaneous bursting rate: stimulation at higher frequencies resulted in a lower fraction of bursts that did occur as a response to stimulation.

We assess changes in the trigger distribution by considering a combined all-electrode criterion for measuring the modification in the trigger distribution that is based on f_n, defined above as the number of bursts triggered by electrode E_n. We define a similarity measure between two trigger distributions $\mathbf{f}' = \{f'_n\}$ and $\mathbf{f} = \{f_n\}$ as their normalized scalar product,

$$S = \frac{\mathbf{f}' \cdot \mathbf{f}}{|\mathbf{f}'| \cdot |\mathbf{f}|}.$$

Here and in the rest of the paper, $|\mathbf{v}|$ stands for the L^2 norm of a vector $\mathbf{v}$.

The similarity S is bounded between 0 and 1, where $S = 1$ means identical trigger distributions, while a similarity of 0 means that all the triggers have been completely replaced by new trigger electrodes. To measure f_n, we used a sliding 8-min interval and then measured the similarity between adjacent 8-min intervals. This gives a good estimator for the changes in the distribution. Before stimulation, S slowly wanders due to the distribution's dynamics, and is close to 0.8–0.9.

Bath stimulation results are presented in figure 5 for the three electrodes with highest leadership score in a typical culture aged 13–14 DIV. After the stimulation, changes in leadership are obvious, with the strongest leader losing its dominance. After another 40 min, this leader regains its standing as the strongest leader, but is far less dominant. In the inset of figure 5, the similarity is depicted for different cultures at different ages. For young cultures (DIV 8–9), the stimulation has, on average, no effect. For DIV 13–14, the similarity drops immediately after the stimulation, reflecting a changing leader distribution. The changes then end within about 40 min, and the similarity goes back to a value of about 0.8–0.9. For the mature culture the drop in similarity was dramatic, but here again within 40 min the distribution stabilized. We note that in contrast to the bath stimulation case, single-electrode stimulation did not result in any modification of the leader distribution (results not shown). This is in line with the results of [22] and [23]. We find that electrodes with high leadership scores undergo stronger changes, but in general, the bath stimulation effects are limited to less than an hour.

3.6. Predictability of activity

One of the key questions raised by the observation of leader electrodes is whether they are passive, merely sensitive probes of the average whole-culture activity or, on the other hand, areas that are active and leading the recruitment of the rest of the culture. One way to discriminate between these alternatives is to identify properties of the burst that correlate with the identity of the leader. In the following paragraphs, we show that the identity of the leader affects the activity following it in both the pre-burst and the burst intervals.

To test the relation between the leaders and the bursts, we analyzed the data in two ways. First, we determine a small number of leader electrodes whose leadership score α is the highest, and for every burst initiated by these leaders, we determine the number of spikes measured in each of the electrodes. Given a leader ℓ, we have a sequence of vectors $\mathbf{e}_{\ell,b}$, whose jth element is the number of spikes that electrode j fired in the bth burst, which was initiated by ℓ. We take the average of the normalized vectors:

$$\mathbf{e}_\ell = \sum_b \mathbf{e}_{\ell,b}/f_\ell,$$

where f_ℓ is again the number of bursts with the leader ℓ. We wish to use these averaged vectors as reference vectors that characterize the different bursts and divide them into different types

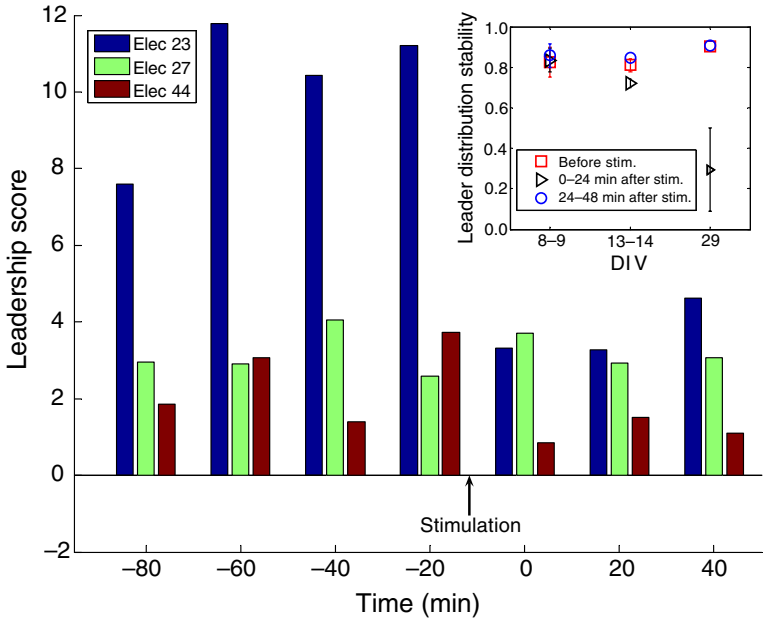

Figure 5. Examples of the effect of bath stimulation on the burst leaders. The leadership score of three electrodes is calculated in consecutive 20 min intervals and plotted as a function of time, for a 13-DIV DF culture. Electrode 23 (blue bars) is the dominant leader before the stimulation, but loses its dominance after the stimulation. Inset: the effect of the stimulation on the dynamics of leader distribution, as exemplified in three culture age ranges ($N = 4, 6, 2$ experiments done on $N = 2, 1, 1$ cultures on DIV 8–9, 13–14 and 29, respectively). The similarity between the leader distributions of adjacent 8-min intervals is averaged over 24 min before the stimulation, 24 min following the stimulation and 24 min later. Before stimulation, the similarity is in the range 0.8–0.9 (red squares). Then, a significant decrease in the leader distribution similarity (p-value $<$ 0.01 or less) is observed for cultures of ages above 13 DIV for the interval immediately following the stimulation, indicating that the stimulation induces changes in the leader distribution (black triangles). Later, the similarity increases, indicating a stabilization of the distribution (blue circles). To allow sufficient statistics, only cultures bursting at least once per minute were considered.

according to their leader. A direct examination of the graph depicting these vectors, plotted versus electrode number, shows that they are practically indistinguishable to the eye (data not shown). However, a prediction can be made for bursts whose trigger has a high leadership score. If $\mathbf{e}$ is the (normalized) vector corresponding to the spike count in one specific measured burst, we form the scalar products $\mathbf{e} \cdot \mathbf{e}_\ell$ and predict that the trigger is that ℓ for which this quantity is largest.

We calculate this predictive product for every burst, and now need to verify that the prediction actually is consistent. Since we also know who was actually the leader of the burst $\mathbf{e}$, say ℓ', we can construct a matrix $A_{\ell',\ell}$ of counts of the various predictions ℓ for the case when ℓ' was the actual leader. In a perfect network, the matrix A would be diagonal, since the

Table 3. Two examples of the correlations between the leader (left column) and the type of burst (top row). Values that are higher than the average by more than 1 SD of their column are underlined. The left matrix is for superepoch 2 of the *CF* culture and the right matrix is for superepoch 2 of a *DF* culture. Note the much higher scores on the diagonal, as well as a small uncertainty for the pair of close-by electrodes (22 and 32) in the left matrix.

	22	32	44	55	57
22	2.43	0.19	1.08	0.87	0.43
32	1.24	0.99	0.59	0.73	0.45
44	1.41	0.47	2.29	0.50	0.33
55	1.18	0.60	0.71	1.78	0.74
57	0.78	0.30	0.54	0.89	2.49

	12	19	40	60
12	3.28	0.29	0.20	0.24
19	0.67	2.40	0.61	0.32
40	0.86	0.16	2.40	0.59
60	1.80	0.26	1.21	0.73

prediction would never be wrong. This is too much to expect for the noisy and untrained neural network we are studying, but the data clearly show a high correlation between the predicted and the true leader. In a totally random situation, the result would be evenly distributed between all the leaders and the relative abundance would be $A_{\ell',\ell}/\sum_{\ell} A_{\ell',\ell} = 1/L$, where L is the number of leaders considered. Thus we show in table 3 the quantities $L\,A_{\ell',\ell}/\sum_{\ell} A_{\ell',\ell}$, and a value > 1 indicates a positive correlation of the prediction.

As mentioned above, bursts belonging to the different types are barely distinguishable on an individual basis, but the differences do show up reliably upon averaging of the large accumulated statistics. The probability of randomly obtaining average values such as the ones depicted in table 3 are extremely small (p-value$< 10^{-15}$), and even if we take only the single columns, still all the calculated p-values are below 10^{-4}. This strengthens the view of the leaders as determining the behavior rather than following it.

A second and different test for the relation between leaders and bursts is done by trying to predict whether an initial activity will develop into a pre-burst or into an aborted burst. In principle, both are a slow initiation process that could lead to a burst, or else die away as an aborted burst. Eytan and Marom [13] showed that these two processes are indistinguishable when averaging over activity. We checked whether the participation of many leaders in the slow initiation process cause it to have a larger probability of turning into a burst than of petering out and ending up as an aborted burst. The prediction is based on the number of leader electrodes (among the five strongest ones) that participate in the first spikes. As shown in figure 6, when more leaders are active in the first 5 spikes, the probability of the activity to lead to a burst becomes significantly greater than the probability to become an aborted burst. The probability of this being random is again extremely small (p-value $< 10^{-15}$).

4. Discussion

Beyond the original observations of Eytan and Marom [13] that revealed the fascinating presence of leaders, we have been able to show that they are a robust and general phenomenon, which is found in a variety of cultures with different feeding protocols. We have also seen that the leaders are both localized and stable. Beyond this, their ubiquity leads us to a fundamental and conceptual issue: the question of how bursts are initiated.

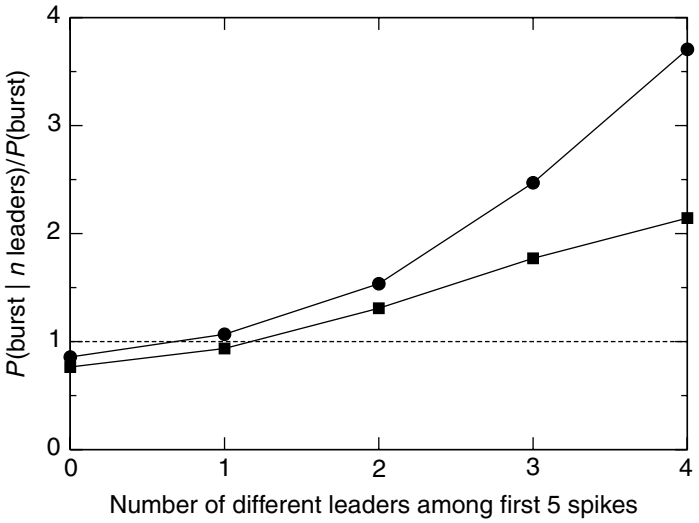

Figure 6. Prediction of burst initiation probability from the occurrence of leaders in the first spikes in the pre-burst or the aborted burst. We obtain a probability ratio by considering the conditional probability to initiate a burst, for any aborted burst or pre-burst, given that there are n different leaders among the first 5 spikes, divided by the probability to see a burst for any aborted burst or pre-burst (we only account for pre-bursts with at least 5 spikes). This ratio of probabilities increases as a function of the number of leaders in the first 5 spikes in the pre-burst. Results are given for superepoch 1 (circles) and superepoch 2 (squares) of *CF*. Given the large number of events considered (tens of thousands), the deviations observed have a p-value $< 10^{-50}$.

We have observed that leaders are omnipresent, appearing in every culture we measured, no matter where the probe electrodes are placed. This leads us to the very reasonable assumption that they are homogeneously dispersed throughout the whole culture, although we have not measured this directly. This assumption is consistent with the fact that even though the location of the electrodes is not expected to be special in any way in all three preparations, still leaders appear in all cultures from the three labs under all conditions. Although the electrodes cover an area that is only a small part of the culture (typically reporting on less than 0.1% of the neurons), they almost invariably succeed in picking up some leaders.

If leading neurons are dispersed all over the culture, then their function is all the more intriguing. We return to the question: are they merely early and passive reporters of activity, or are they active initiators of the burst? Two observations make us conjecture that leaders not only report on the burst, but are active in causing it.

The first is the locality of activity in the pre-burst, indicating a recruitment process [12]. The transfer of information from the leader to its surrounding neurons is a preface to the transition of the whole network to a full burst. This is reminiscent of a similar recruitment process around BIZ in 1D networks, in which a transition from low-amplitude, localized activity to higher-amplitude, fast propagating activity was observed [8], that is related to the buildup of synchrony in neural firing [15]. If the bursts were coming from outside the monitored area, then we would expect them to appear abruptly, with no pre-burst and no gradual growth like the one we observe.

So, although we only observe a small part of the culture, leaders are clearly identified in the field of observation for most of the bursts, indicating that the burst generation must have a local component in its genesis.

The second observation is the predictive power of the leaders as to the 'character' of the burst. Several groups have reported on the existence of a limited number of firing patterns in the bursts. In [4], Maeda *et al* observed propagation of spontaneous activity across their 10 mm array. The direction of propagation of the spontaneous activity, as well as the spontaneous activity initiation area, changed from burst to burst. In addition [4, 21], they reported that activity evoked by local electrical stimulation typically started earlier in electrodes closer to the stimulating electrode. van Pelt *et al* [10] reported that the firing rate of each electrode peaked with a characteristic time difference relative to the peak of the whole-culture spontaneous firing rate. Hence, a subset of the electrodes tends to fire earlier than the whole culture. Segev *et al* [24] showed that the spontaneous bursts can be clustered into 2–3 groups, based on the electrodes' firing rate profiles as a function of time.

We have seen that the spiking pattern (number of spikes per electrode) within the burst provides a signature that suffices to statistically identify its leader. Similarly, the firing pattern of leaders in the first few spikes of the aborted burst or the pre-burst allows a prediction as to whether a burst will form or not. We conclude from this that a relationship must exist between a burst and local leaders, emphasizing again that this is by no means just a statistical abundance of spiking by the leaders, but a sign of signaling between the leader, the exterior parts of the sample and the burst generation.

The final question that arises is: what then do these leaders have as input that makes them fire first? A sparse subset of self-firing neurons [25] may exist, and the leaders may include such neurons, or else they may be well connected to other neurons that are self-firing. At any rate, the dominant signal inputting on a given neuron is usually thought to arise from the self-firing of neurons rather than from environmental cues (such as fluctuations in the amount of ions in the surrounding fluid). The reason that the leaders are first to fire may be that they have the most inputs, or that they are more sensitive to excitation. Recall, however, that they do not fire particularly often.

We can think of three scenarios for how the leaders are excited. In the simplest case, one leader in the whole culture is self-excited, or else stimulated by a localized low-level background activity. By becoming very active, it will recruit first its nearby environment and then gradually the rest of the network through a percolation process. This scenario is rejected within our picture: we have argued that several leaders are being excited concurrently, otherwise we would not have seen leaders in the small region in which we measure.

The second scenario involves a number of leaders being excited simultaneously by a widespread low-level noise that can activate many of the leaders in parallel. In this case, they each excite a region around them, and these coalesce at random as the whole network bursts. The argument against this scenario is that we would not expect then a variability in the signature of the burst, since all bursts would evolve essentially in the same route, with the leaders being excited first and then recruiting their respective neighborhoods.

The third, most tentative yet most attractive scenario posits the existence of an underlying 'sub-network' connecting potential leaders. Their activation is triggered by the noise, but here a small amount of background firing can suffice to set off the burst, since the leaders first communicate among themselves and only then initiate the activity of other leaders. Variations in the noise that initially sets off the network could then cause variation in the response of the

leader sub-network, affecting the parts of it that are recruited. This, in turn, reflects on the details and signature of the burst.

This scenario is particularly intriguing since it implies a stochastic percolation behavior in the sub-network of the leaders which, once they have fired, act as nucleation sites for the whole network. Perhaps one could answer the questions raised in this discussion experimentally, first measuring passively and identifying leaders and then intervening (e.g. chemically) and selectively suppressing the activity of the neurons near those electrodes with leader properties.

Acknowledgments

We thank Steve Potter for making the data from his laboratory available to us. EM and SJ thank Menahem Segal for advice, and SM thanks Vladimir and Elleonora Lyakhov for technical assistance. JPE and CZ were supported by the Fonds National Suisse, SM by a grant from the Israel Science Foundation and EM and SJ by grants from the Israel Science Foundation, the Minerva Foundation (Germany) and the Clore Center for Biological Physics. JPE and CZ are grateful for the hospitality of the Minerva Einstein Center.

References

[1] Marom S and Shahaf G 2002 Development, learning and memory in large random networks of cortical neurons: lessons beyond anatomy *Q. Rev. Biophys.* **35** 63–87
[2] Eckmann J-P, Feinerman O, Gruendlinger L, Moses E, Soriano J and Tlusty T 2007 The physics of living neural networks *Phys. Rep.* **449** 54–76
[3] Tscherter A, Heuschkel M O, Renaud P and Streit J 2001 Spatiotemporal characterization of rhythmic activity in rat spinal cord slice cultures *Eur. J. Neurosci.* **14** 179–90
[4] Maeda E, Robinson H P and Kawana A 1995 The mechanisms of generation and propagation of synchronized bursting in developing networks of cortical neurons *J. Neurosci.* **15** 6834–45
[5] Droge M H, Gross G W, Hightower M H and Czisny L E 1986 Multielectrode analysis of coordinated, multisite, rhythmic bursting in cultured CNS monolayer networks *J. Neurosci.* **6** 1583–92
[6] Wagenaar D A, Pine J and Potter S M 2006 An extremely rich repertoire of bursting patterns during the development of cortical cultures *BMC Neurosci.* **7** 11
[7] Latham P E, Richmond B J, Nirenberg S and Nelson P G 2000 Intrinsic dynamics in neuronal networks. I. Theory *J. Neurophysiol.* **83** 808–27
[8] Feinerman O, Segal M and Moses E 2005 Signal propagation along unidimensional neuronal networks *J. Neurophysiol.* **94** 3406–16
[9] Feinerman O, Segal M and Moses E 2007 Identification and dynamics of spontaneous burst initiation zones in uni-dimensional neuronal cultures *J. Neurophysiol.* **97** 2937–48
[10] van Pelt J, Vajda I, Wolters P S, Corner M A and Ramakers G J 2005 Dynamics and plasticity in developing neuronal networks in vitro *Prog. Brain. Res.* **147** 173–88
[11] Darbon P, Scicluna L, Tscherter A and Streit J 2002 Mechanisms controlling bursting activity induced by disinhibition in spinal cord networks *Eur. J. Neurosci.* **15** 671–83
[12] Yvon C, Rubli C and Streit J 2005 Patterns of spontaneous activity in unstructured and minimally structured spinal networks in culture *Exp. Brain. Res.* **165** 139–51
[13] Eytan D and Marom S 2006 Dynamics and effective topology underlying synchronization in networks of cortical neurons *J. Neurosci.* **26** 8465–76
[14] Papa M and Segal M 1996 Morphological plasticity in dendritic spines of cultured hippocampal neurons *Neuroscience* **71** 1005–11

[15] Jacobi S and Moses E 2007 Variability and corresponding amplitude-velocity relation of activity propagating in one-dimensional neural cultures *J. Neurophysiol.* **97** 3597–606
[16] Potter S M and DeMarse T B 2001 A new approach to neural cell culture for long-term studies *J. Neurosci. Methods* **110** 17–24
[17] Potter S M 2001 Distributed processing in cultured neuronal networks *Prog. Brain Res.* **130** 49–62
[18] Eckmann J-P, Moses E and Sergi D 2004 Entropy of dialogues creates coherent structures in e-mail traffic *Proc. Natl Acad. Sci: USA* **101** 14333–7
[19] Bartlett W P and Banker G A 1984 An electron microscopic study of the development of axons and dendrites by hippocampal neurons in culture. I. Cells which develop without intercellular contacts *J. Neurosci.* **4** 1944–53
[20] Kriegstein A R and Dichter M A 1983 Morphological classification of rat cortical neurons in cell culture *J. Neurosci.* **3** 1634–47
[21] Maeda E, Kuroda Y, Robinson H P C and Kawana A 1998 Modification of parallel activity elicited by propagating bursts in developing networks of rat cortical neurons *Eur. J. Neurosci.* **10** 488–96
[22] Wagenaar D A, Pine J and Potter S M 2006 Searching for plasticity in dissociated cortical cultures on multi-electrode arrays *J. Negat. Results BioMed.* **5** 16
[23] Eytan D, Brenner N and Marom S 2003 Selective adaptation in networks of cortical neurons *J. Neurosci.* **23** 9349–56
[24] Segev R, Baruchi I, Hulata E and Ben-Jacob E 2004 Hidden neuronal correlations in cultured networks *Phys. Rev. Lett.* **92** 118102
[25] Latham P E, Richmond B J, Nirenberg S and Nelson P G 2000 Intrinsic dynamics in neuronal networks II. Experiment *J. Neurophysiol.* **83** 828–35